J Physiol (2003), **550.3**, *pp.* 667–677

DOI: 10.1113/jphysiol.2003.039321
www.jphysiol.org

Journal of Physiology

Sugar transport by mammalian members of the SLC26 superfamily of anion–bicarbonate exchangers

J-M. Chambard and J. F. Ashmore

Department of Physiology, University College London, Gower Street, London WC1E 6BT, UK

The mammalian cochlea contains a population of outer hair cells (OHCs) whose electromotility depends on an assembly of 'motor' molecules in the basolateral membrane of the cell. Named 'prestin', the molecule is a member of the SLC26 anion transporter superfamily. We show both directly and indirectly that SLC26A5, rat prestin, takes up hexoses when expressed in several cell lines. Direct measurements of labelled fructose transport into COS-7 cells expessing prestin are reported here. Indirect measurements, using imaging techniques, show that transfected HEK-293 or CHO-K1 cells undergo reversible volume changes when exposed to isosmotic glucose–fructose exchange. The observations are consistent with the sugar transport. A similar transport was observed using a C-terminal green fluorescent protein (GFP)-tagged pendrin (SLC26A4) construct. Cells transfected with GFP alone did not respond to sugars. The data are consistent with fructose being transported by prestin with an apparent K_m = 24 mM. From the voltage-dependent capacitance of transfected cells, we estimate that 250 000 prestin molecules were present and hence that the single transport rate is not more than 3000 fructose molecules s^{-1}. Comparison of the transfected cell swelling rates induced by fructose and by osmotic steps indicates that water was co-transported with sugar. We suggest that the structure of SLC26 family members allows them to act as neutral substrate transporters and may explain observed properties of cochlear hair cells.

(Resubmitted 14 January 2003; accepted after revision 30 April 2003; first published online 30 May 2003)
Corresponding author J. F. Ashmore: Department of Physiology, University College London, Gower Street, London WC1E 6BT, UK. Email: j.ashmore@ucl.ac.uk

The SLC26 gene family (solute carrier family 26) comprises nine mammalian genes encoding anion transporter-related proteins. In humans, nine tissue-specific genes of the SLC26 family have been cloned so far (Lohi *et al.* 2000; Waldegger *et al.* 2001; Kim *et al.* 2002; Lohi *et al.* 2002) and homologues have been identified in other genomes. When expressed in oocytes, these proteins transport chloride, iodide, bicarbonate, oxalate, and hydroxyl anions with different specificity. The SLC26A2 and SLC26A3 genes are mutated in disease states such as diastrophic dysplasia and congenital chloride diarrhoea respectively. The SLC26A6 protein is expressed at highest levels in the kidney and the pancreas. The newest member, SLC26A8 or TAT1, has been shown to act as a sulfate transporter in human male germ cells. SLC26A7 to A9 show tissue-specific expression in the kidney, testis and lung, respectively (Lohi *et al.* 2002).

SLC26A4 and SLC26A5 are both expressed in the inner ear. SLC26A4, or pendrin, is detected throughout the endolymphatic duct and sac, in distinct areas of the utricule and saccule, and in the external sulcus region within the cochlea (Everett *et al.* 1999). SLC26A5, or prestin, has been cloned from gerbil (Zheng *et al.* 2000) and rat (Ludwig *et al.* 2001) and shown to act as a motor protein of cochlear outer hair cells (OHCs). Prestin is best described as a transporter with a low efficiency transport cycle. It undergoes conformational changes under the influence of membrane voltage. Intracellular anions act as the sensors (Oliver *et al.* 2001).

In OHCs of the mammalian cochlea, there is physiological evidence that some sugars, and fructose in particular, can be taken up by a mechanism in the lateral membrane (Géléoc *et al.* 1999; Ashmore *et al.* 2000). The functional and immunohistochemical profile best match an isoform of the hexose transporter GLUT5 which has a substrate preference for fructose. In order to study this property of sugar transport, we used transfected cell lines as an expression model to elucidate the protein involved. We describe here transport properties of the rat homologue of prestin and the human homologue of pendrin by studying the biophysical and cellular properties following sugar replacement in the bathing solution. We find that both prestin and pendrin transport fructose, and derive an estimate for the rate of this non-standard entry route of sugar substrates into hair cells.

METHODS

Cell culture and transfection

Human embryonic kidney (HEK)-293, COS-7 and Chinese hamster ovary (CHO)-K1 cells were grown at 37 °C and in 5 % CO_2 in Dulbecco's modified Eagle's medium (DMEM) supplemented with 10 % fetal calf serum. Cells were split weekly when confluent. They were transfected directly in a 75 cm^3 flask (Falcon) using LipofectAmine (Life Technologies, Gaithersburg, MD, USA) according to the manufacturer's recommendations. A plasmid coding for the six transmembrane KCNQ4 potassium channel (a gift from A. Tinker, Department of Clinical Pharmacology, UCL, UK) was used as a control for expression of a membrane protein. Plasmids containing rat prestin (a gift from B. Fakler, Department of Physiology II, University of Freiburg, Germany) and human pendrin (a gift from R. Trembath, Department of Genetics, University of Leicester, UK) cDNAs were both driven by cytomegalovirus promoter. Prestin cDNA was ligated into the eukaryotic expression plasmid vector pBK-CMV (Stratagene) with the GFP-mut3 coding sequence fused to the 3′ end of the prestin sequence (see Ludwig *et al.* 2001).

The pendrin cDNA sequence was subcloned into the *Xho* I–*Kpn* I site of pEGFP-N1 (Clontech) using standard cloning protocols, to produce a construct encoding a carboxy-terminal GFP–pendrin fusion protein.

Twenty-four hours after transfection, the cells were trypsinised. Trypsinisation followed transfection in order to increase the number of isolated cells we used in this study. Cells were plated on 35 mm glass-bottomed microwell dishes (MatTek, MA, USA) for imaging over the subsequent 72 h. All experiments were carried out at room temperature.

Solutions

For imaging experiments, the cell medium was replaced by an external solution of standard saline containing (mM): NaCl 135, KCl 4, $CaCl_2$ 1, Hepes 5 and D-glucose 30. The pH was set at 7.2 ± 0.2. At least three measurements of osmolality were performed before and after each experiment. Average values of osmolality were found to be 320 ± 1 mosmol kg^{-1}. All chemicals and media were supplied by Sigma unless otherwise stated.

A pipette, pulled on a programmable puller (PIP5, HEKA) from 1.2 mm o.d. borosilicate glass capillaries (GC120TF, Clark Electromedical Instruments, UK) to a tip diameter of 1–2 μm, was filled with the test solutions. The puff pipette was placed 100 μm from the recorded cell and pressure was applied by a pneumatic injection system (PV800, World Precision Instruments, NH, USA). Fructose solutions were applied at different concentrations in standard saline solution, adjusted to 320 ± 1 mosmol kg^{-1} with the corresponding sugar. To compensate, NaCl concentration was reduced to 125 mM to make the 50 mM fructose solution. The hypo- and hyperosmotic solutions were made with the appropriate concentration of the desired sugar.

The data for the initial rate of change in the diameter of the cell (V_i) were fitted by Michaelis–Menten kinetics for a saturable uptake mechanism:

$$V_i = \frac{V_{max}[s]}{K_m + [s]}, \quad (1)$$

with V_{max} the maximum rate, [s] the sugar concentration and K_m the half-saturating concentration.

In order to determine the effect of salicylate on sugar transport, the external 30 mM glucose solution containing 10 mM salicylate was replaced by a solution containing 30 mM fructose and 10 mM salicylate. 4,4′-Diisothiocyanostilbene-2,2′-disulfonic acid (DIDS), a blocker of Cl^-–HCO_3^- exchange, was added directly to the bathing and perfusing solution.

Measurement of [^{14}C]fructose uptake

[^{14}C]Fructose (Amersham) was used as a probe in a transport assay. COS-7 cells were used in this experimental approach because approximately 70 % of these cells exhibited transfection. Cells were grown on 6-well dishes and transfected with a plasmid coding for GFP, or co-transfected with GFP and pcDNA3 carrying cDNA coding for prestin. After removal of the culture medium, cells were incubated for 10 min at 37 °C in the standard solution containing 30 mM glucose. To demonstrate loading, glucose was replaced with 30 mM fructose and 150 μM [^{14}C]fructose. After 5 min, cells were washed with cold fructose at 0 °C and solubilised with PBS containing 5 % Triton-X 100. The radioactivity was measured using a scintillation counter.

Imaging

Images were captured at 0.2 Hz by a Hamamatsu C4880 cooled CCD camera with 12-bit fluorescence resolution using AQM software (Kinetic Imaging, Liverpool, UK). GFP fluorescence was identified using an FITC filter set in an inverted microscope (Axiovert S-100, Zeiss, Germany). All imaging was carried out using a × 40 1.3 NA FLUAR objective. The probe was excited at 440 nm and emission measured at 530 nm. The intensity of the exciting light was adjusted wherever possible to minimise photobleaching. Fluorescence imaging of the cell boundary was found preferable to bright field identification of the boundary because it allowed simultaneous identification of transfected cells and high spatial resolution measurements. Untransfected cells were imaged using differential interference contrast (DIC) optics alone for experiments on water movement. This procedure may produce errors for small diameter changes.

Analysis of each recorded image was carried out using a number of techniques. It was found more convenient to image fluorescent boundaries than bright field image boundaries as the transfected cells were already identified by their fluorescence. Cell diameter changes were made by following the movement of the GFP fluorescent cell membrane along a cell diameter using software developed using Matlab (Mathworks, Natick, MA, USA). Cell areas were independently estimated by measuring the area in each frame using Metamorph software (Universal Imaging, West Chester, PA, USA). For a spherical cell, the following relation holds between cell diameter D, cell area A and cell volume V:

$$\frac{\delta V}{V} = \frac{3}{2}\frac{\delta A}{A} = 3\frac{\delta D}{D}, \quad (2)$$

so that in principle, cell volume changes can be determined from cell diameter changes.

A first indicator that the cell was an approximately spherical object was obtained from capacitance measurements. The linear capacitance of a population of HEK-293 cells was determined to be 21 ± 4 pF (n = 50). Assuming a membrane capacitance of 1 μF cm^{-2}, the diameter of a spherical cell with this capacitance would be 25.9 μm; the measured diameter of the same population of cells was 21 μm, suggesting that the selected cells had an approximately spherical geometry.

To confirm the spherical geometry of the studied cells, a three-dimensional (3-D) reconstruction of a prestin-transfected cell was imaged by conventional laser-scanning confocal microscopy using a Zeiss LSM 510 confocal microscope with a × 63 LWD WI objective (data not shown). Using reconstruction in the *z*-direction, the cell was observed to be spherical in shape. Thus eqn (2) allows an effective inference of the cell volume changes.

Osmotic permeability

The volume flow of water into the cells, $J_v = dV/dt$, was determined from the rising portion of the cell volume change measured as described above. For changes in osmotic pressure across the cell membrane, the osmotic water permeability (L_p) is proportional to J_v through $L_p = J_v/(SV_W\Delta\pi)$ where S is the surface area of the cell, $V_W = 8\ cm^3\ mol^{-1}$ is the partial molar volume of water and $\Delta\pi$ is the difference in osmotic pressure (in osmol (kg H_2O)$^{-1}$) across the cell membrane (Loo *et al.* 1999). In the experiments here we take, to a good approximation, $\Delta\pi = \Delta C$, the difference in solute concentration (in mol l^{-1}). In the calculations, the cell area is taken to be that of a sphere 20 μm across.

Electrophysiology

Voltage-dependent capacitance was measured by using a phase-tracking technique (Neher & Marty, 1982; Gale & Ashmore, 1997). After manual compensation of membrane capacitance (C_m), lock-in phase angles yielded signals proportional to the change in C_m. The capacitance output was calibrated by a 100 fF dither in the capacitance compensation setting. A command sinusoid with a frequency of 1100 Hz was used and summed with a ramp ranging between −150 and +50 mV as the stimulus. Scaled capacitance traces as well as the conductance signal and steady-state current induced by the voltage ramp were plotted *versus* the membrane voltage. Capacitance was fitted with the derivative of a first order Boltzmann function:

$$C(V) = C_{lin} + \frac{Q_{max}}{\alpha\exp\{(V - V_{1/2})/\alpha\}\{1 + \exp(-(V - V_{1/2})/\alpha)\}^2}, \quad (3)$$

where C_{lin} is linear membrane capacitance, V is membrane potential and Q_{max} is maximum charge moved through the membrane electrical field. The voltage at half-maximum charge transfer is $V_{1/2}$, and $\alpha = (ze/k_BT)^{-1}$ is the slope factor of the voltage dependence of charge transfer, k_B is Boltzmann's constant, T is absolute temperature, z is valency and e is electronic charge. Fits to the data employed a Levenberg–Marquardt algorithm. All data are given as means ± S.D.

RNA extraction and RT-PCR

Total RNA was extracted from hamster testes, CHO-K1 and HEK-293 cells using a RNeasy kit (Qiagen) and resuspended in water, and its concentration was estimated by optical density at 260 nm. Adult hamsters were killed by rapid cervical dislocation in accordance with the UK Animals (Scientific Procedures) Act 1986. The hamster GLUT5 sequence is unknown and, therefore, three pairs of mouse primers designed to detect mGLUT5 were tested against mRNA from hamster testes (testes are known to express GLUT5 in other species; Burant *et al.* 1992). One of these primer pairs identified a specific 220 bp cDNA. The primer sequences were: 5′-AACGCTCATCGCTGCCTT-3′ and 5′-CTC-GTGGTTGGAAACTTGGT-3′. Human GLUT5-specific primers 5′-AGCTGCTGTCCATCATCGTC-3′ and 5′-CGATGCTGATGT-ATGGCATC-3′ were also synthesised (Kurata *et al.* 1999) by Sigma Genosys, and generated a single band at 302 bp. cDNA was synthesised by reverse transcriptase for 30 min at 42 °C and amplified by 35 cycles of 45 s at 94 °C, 45 s at 55 °C (58 °C for human primers) and 30 s at 72 °C and a final extension at 72 °C for 7 min. The products were separated and visualised by ethidium bromide staining on a 2 % agarose gel.

RESULTS

The C-terminal GFP-tagged rat prestin construct was expressed in HEK-293, COS-7 and CHO cells. As prestin is a membrane protein, cells successfully transfected showed the GFP tag predominantly localised at the plasma membrane (Fig. 1*A*). When the GFP was expressed alone in the same cell line, it was localised in the cytoplasm and not in the membrane (Fig. 1*B*). The fluorescent tag unambiguously allowed cells to be identified and their membrane movements to be quantified.

Prestin transports labelled [^{14}C]fructose

To measure fructose transport directly, radiolabelled fructose uptake was measured (Asano *et al.* 1989). In view of their high transfection levels, COS-7 cells were used in this part of the study. Cells were transfected with GFP alone or co-transfected with GFP and prestin. Cells were incubated with 30 mM glucose solution for 10 min and then with the glucose replaced by 30 mM fructose and 150 μM of [^{14}C]fructose for 5 min. A standard volume of cells transfected with GFP and prestin yielded a count of

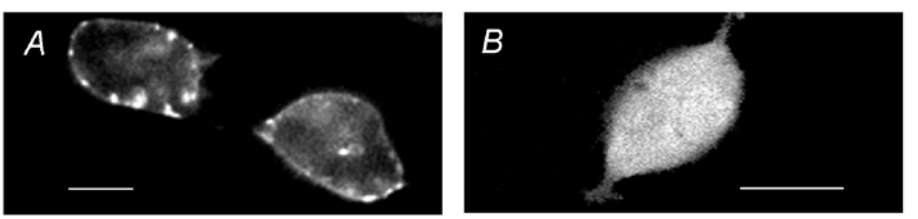

Figure 1. Immunofluorescence of transfected cells

A, HEK-293 cell expressing the green fluorescent protein (GFP)-tagged prestin protein. As prestin is a membrane protein, the GFP tag is predominantly localised at the plasma membrane. *B*, HEK-293 cell expressing GFP alone; GFP was localised in the cytoplasm and not in the membrane. Scale bar, 10 μm.

35 907 ± 4146 d.p.m. (n = 3). As a control for background, cells transfected with GFP alone yielded a count of 6083 ± 424 d.p.m. (n = 3). Thus fructose uptake increased by approximately 6-fold in cells expressing prestin.

Prestin transport of sugar measured by image analysis

In order to quantify prestin sugar transport, an indirect measurement, based on cell swelling, was used. If a solute is transported preferentially into a cell, there should be an increase in cell volume as water flows in to maintain osmotic balance. Sugar transport in HEK-293 cells expressing prestin was investigated by analysing the changes in cell diameter and area when glucose was replaced isosmotically in the external bathing medium. Such prestin-transfected cells exhibited a significant change in the observed cell diameter and area. Figure 2*A* shows the change in cell diameter of a typical prestin-expressing HEK-293 cell. Comparable cell swelling was observed in prestin-expressing CHO cells (Fig. 5*B*). When HEK-293 cells were transfected with the GFP construct alone, there was no change in diameter or area when 30 mM fructose was substituted for 30 mM glucose in the external media (data not shown).

In order to eliminate the possibility that transport occurred via a pathway activated by expression of membrane proteins, a membrane protein not related to the SLC26 family, a potassium channel, was used as a control expressed protein. Fructose replacements were made on HEK-293 cells expressing this membrane protein. Independent whole-cell recording showed that this protein was functionally present in the membrane. There was no change in diameter or area of these transfected cells (data not shown).

To quantify the diameter change, a profile was drawn across the cell and the positions of the fluorescent boundaries measured. The positioning of the fluorescence profile was found not to be critical providing that approximately the widest dimension was measured. The average diameter for the studied cells was 20 μm. The cell

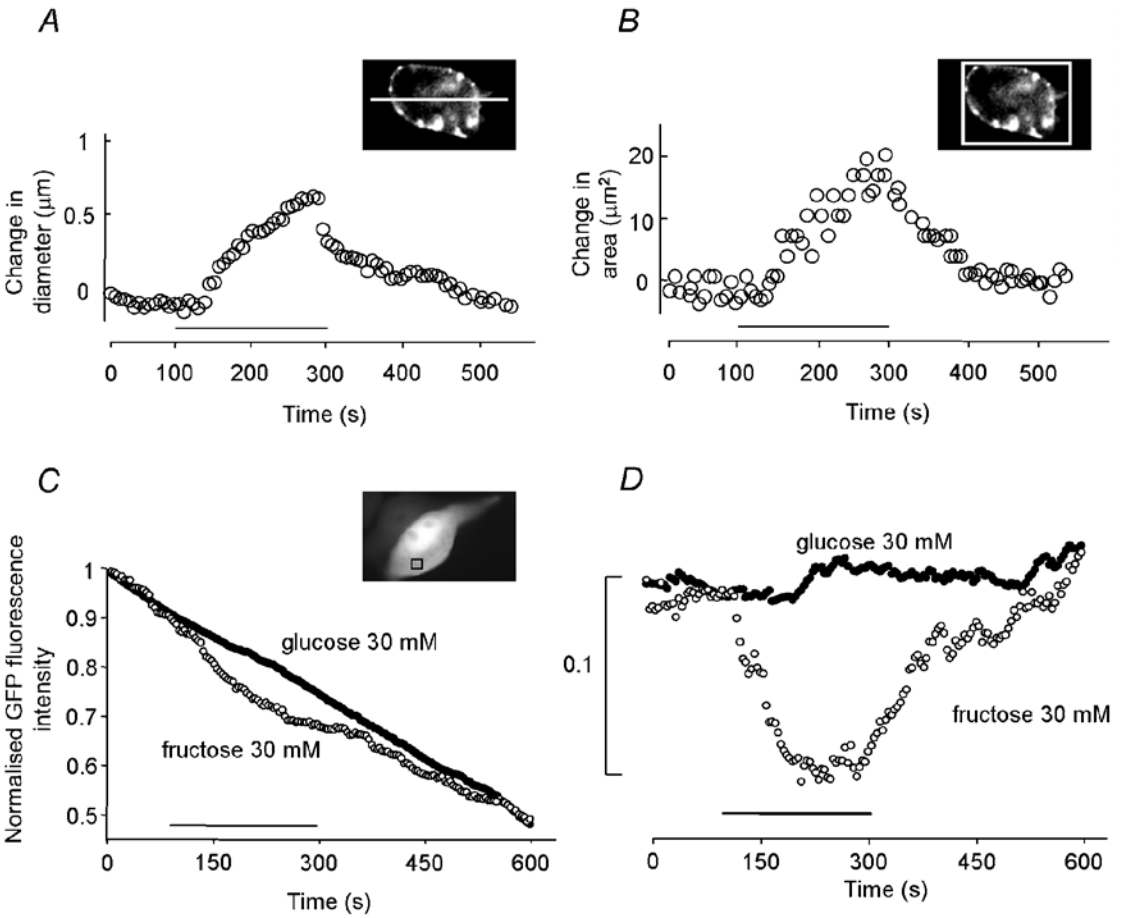

Figure 2. Diameter, area and fluorescence change during sugar application on HEK-293 cells expressing rat prestin

Measurements of cell diameter (*A*) or area change (*B*) using two different techniques (see Methods). The bar indicates the sugar application. *C*, change in the GFP fluorescence of a region of interest contained entirely within the cytoplasmic region (as indicated) during application of 30 mM fructose (○) but not 30 mM glucose (●). Traces have been normalised to the maximum GFP fluorescence intensity at the beginning of each recording. *D*, same data as in *C* but with linear subtraction for photobleaching.

increased by 0.5–0.8 μm in diameter, or equivalently by 2.9 ± 1.7 % (mean ± S.D., $n = 20$). As a check, cell areas were also measured (Fig. 2*B*). They were found to increase by between 15 and 25 μm^2. The equivalent percentage area increase was 5.9 ± 3.6 % ($n = 20$). Thus cells behaved as if they were approximately spherical (see Methods). On return to the original bathing medium, the cells returned to their original size (Fig. 2*A* and *B*).

In order to confirm that the increase in diameter and area was due to water flow into the cell, the fluorescence intensity was measured in an area in the cytoplasm before, during and after sugar application for cells co-transfected with GFP and prestin ($n = 5$). Figure 2*C* shows the time course of the change in GFP fluorescence intensity in the cytoplasm during different sugar application for a representative cell. Application of 30 mM glucose caused only a linear decrease due to photobleaching of the fluorescent probe (~50 % of the intensity in 12 min). Application of 30 mM fructose produced a decrease that can be explained by a dilution of the signal following water influx. Figure 2*D* shows the difference between the traces and the time course of the fluorescence dilution after subtraction of photobleaching as a linear function of time. An area excluding the nucleus and other organelles was used as a reference to perform this subtraction. These data clearly demonstrate that the swelling of the cell during the sugar transport is due to a water flow.

Using the protocol for measuring diameter change, a series of experiments were carried out in which external glucose was replaced by different concentrations of fructose.

Firstly, we found that there was no significant difference in the diameter and area changes between cells when the GFP–prestin construct was used and when cells were co-transfected with prestin and GFP (Fig. 3*A*). The GFP tag did not interfere with the sugar transport.

Secondly, Fig. 3*B* illustrates the percentage change in area of HEK-293 cells on replacement of external glucose by 5, 20, 30 and 50 mM fructose solution. The observed swelling showed characteristics of a saturable uptake process. Thus 5 mM fructose application produced a 2.0 ± 0.8 % ($n = 12$) increase in cell area. An increase in concentration of external fructose to 20 and 30 mM resulted in a subsequent increase in swelling, with increases in cell area of 3.4 ± 1.2 % ($n = 9$) and 5.9 ± 3.6 % ($n = 20$), respectively. On application of 50 mM fructose the area increased by 5.8 ± 2.5 % ($n = 12$). This was not a significant rise above that obtained with 30 mM fructose.

Figure 4*A* shows the time course of the cell swelling at each fructose concentration. The initial rate, V_i, of diameter increase during the first 20 s after the beginning of the fructose application, was used to fit Michaelis–Menten kinetics for a saturable uptake mechanism (Fig. 4*B*). Based

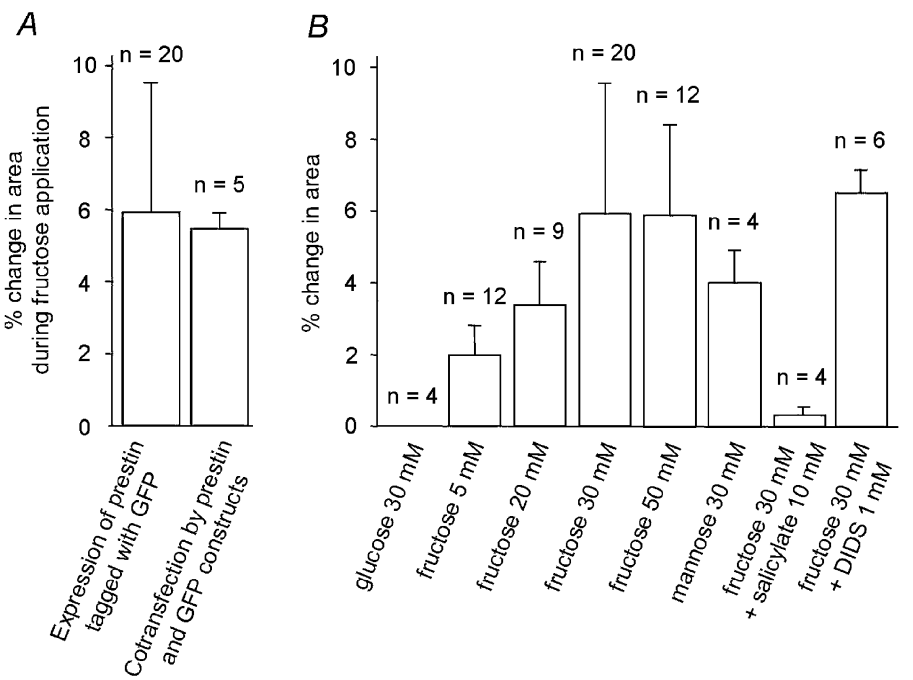

Figure 3. Sugar uptake by HEK-293 cells expressing rat prestin

A, the GFP tag did not interfere with fructose transport. *B*, glucose, fructose and mannose uptake by HEK-293 cells expressing prestin, measured by change in area. Area change after 150 s of isosmotic replacement of 30 mM glucose by the same solution, fructose at increasing concentration (5, 20, 30 and 50 mM) or 30 mM mannose is shown. The last two columns show the effect of two compounds added to 30 mM fructose: 5 mM salicylate (a blocker of OHC electromotility) and 1 mM DIDS (a blocker of the chloride–bicarbonate exchanger).

on the curve fitted to the data set, the estimated value for K_m was 24 mM, and V_{max} was 0.04 % s^{-1}. These values show that these cells reached a steady-state diameter in approximately 2.9/0.04 = 75 s after sugar exposure. For comparison, when OHCs were presented with fructose they lengthened in approximately 5 s. There was no evidence for a baseline exchange of glucose across the cell membrane as no change in area was detectable when 30 mM sucrose was replaced by 30 mM glucose in the bathing medium (data not shown).

The specificity of sugar transport was studied by replacing 30 mM glucose in the external medium with other hexose sugars. In OHCs there is little change in cell length when glucose is replaced by sucrose or mannose (Géléoc *et al.* 1999). However, an application of 30 mM mannose produced a 4.1 ± 1.0 % increase in cross-sectional cell area (n = 4). Thus mannose transport occurs in HEK-293 cells transfected with rat prestin and we suggest that prestin can transport hexose sugars but with a weak substrate specificity for fructose.

Effect of salicylate as a blocker of fructose transport

Salicylate is a known blocker of charge movement in OHCs (Tunstall *et al.* 1995) and inhibits fructose transport in OHCs (Ashmore *et al.* 2000). There is also evidence that it behaves as a competitive inhibitor of chloride binding in the prestin molecule (Oliver *et al.* 2001). To test the effect of salicylate on rat prestin-transfected HEK-293 cells, isosmotic replacement of glucose with fructose was carried out in the presence of 10 mM salicylate. The cell medium was replaced by 30 mM glucose solution containing 10 mM salicylate and allowed to stand for 5 min. On application of 30 mM fructose in the presence of 10 mM salicylate, there was no significant change in cell area. Thus salicylate blocked the fructose-induced cell volume change.

Estimation of the sugar transport rate per prestin molecule

The number of copies of prestin protein expressed per cell can be estimated from electrical measurements. The maximum non-linear capacitance (C_{max}) of the cell is related to the number N_a of charges moved by:

$$N_a = \frac{4\alpha C_{max}}{e}, \quad (4)$$

where α and e have the usual meanings as in eqn (3).

Capacitance measurements were carried out only in the CHO cells as the HEK-293 cells expressed a leakage current that was too large for effective extraction of the C_{max}. However, the data from transfected CHO cells and HEK-293 cells showed identical rates of uptake of mannose and fructose (Fig. 5*B*).

As expected, CHO cells expressing rat prestin exhibited a bell-shaped voltage-dependent capacitance when tested with voltage ramps running from −150 to +50 mV (Fig. 5*C*). This electrical signature was fitted with the derivative of a first-order Boltzmann function (eqn. (2)) yielding values for $V_{1/2}$ = −89.9 ± 8.4 mV and α = 38.9 ± 3.3 mV (n = 3). There was no non-linear capacitance measured in CHO cells transfected with the GFP construct alone. Hence, using a measured value of C_{max} = 0.4 pF (Fig. 5*C*) and eqn (4), and making the assumption that there is one charge movement per prestin molecule, we estimate that there were N_a = 250 000 prestin molecules expressed per cell.

Using eqn (2), the initial rate of volume change per cell when exposed to 30 mM fructose (Fig. 4*B*) was:

$$(d/dt)(\delta V/V) = 3 \times 0.03/100 = 0.001\ s^{-1}$$

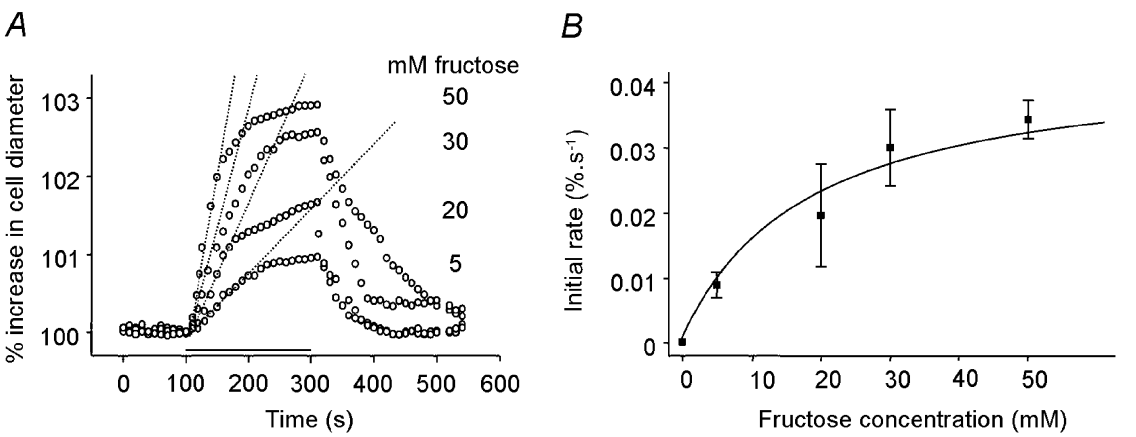

Figure 4. Kinetics of fructose uptake by HEK-293 cells transfected with rat prestin

A, changes in diameter following sugar application at different concentrations. The solid horizontal bar indicates the timing of the isosmotic replacement of glucose by fructose. Fructose was applied at 5 mM (n = 12), 20 mM (n = 9), 30 mM (n = 20) and 50 mM (n = 12). The dashed line superimposed on the traces is a linear fit through the rising phase of the volume response. *B*, initial transport rate estimated by a linear fit between t = 0 s and t = 20 s after the beginning of the application. Data were fitted by eqn (3) with V_{max} = 0.04 % s^{-1} and K_m = 24 mM.

This value is about two orders of magnitude less than that found in adult OHCs (Ashmore *et al.* 2000). Since the experiment used isosmotic replacement of 30 mM of a non-transported sugar (glucose) with a transported sugar (fructose), we can calculate the number of fructose molecules transported on the assumption that the fructose entering the cell neither concentrated nor diluted the cell contents. For a spherical cell of 4 pl in volume (diameter 20 μm), the transport rate for fructose was:

$$0.001 \times 4 \times 10^{-12} \times 0.320 = 1.3 \times 10^{-15} \text{moles s}^{-1},$$

or equivalently 7.7×10^{8} fructose molecules s^{-1}. Using the electrophysiological estimates for the number of prestin molecules per cell, we deduce that the initial rate of transport per cell was 3080 fructose molecules (prestin molecule)$^{-1}$ s^{-1}.

Water co-transport with fructose

The experiments described so far indicate that the cell volume changed because water flowed into the cell to maintain osmotic balance. The following experiments suggest that water was carried with fructose through the prestin transport pathway. Such coupled transport has been described for other transport systems (e.g. Fischbarg *et al.* 1990; Zeuthen *et al.* 2001). Figure 6 shows the reversible swelling of a prestin-transfected cell produced by a hypo-osmotic challenge. Cell volumes were normalised to unity at the start of the experiment. Transfected cells were bathed in standard solution containing 30 mM glucose (320 mosmol kg^{-1}), which was then made hypo-osmotic by removing the glucose (290 mosmol kg^{-1}, ●). After 200 s the cells had increased in volume by 5.2 ± 1.0 % (n = 4). In contrast to isosmotic replacement experiments, cells showed only a partial volume recovery on return to 30 mM glucose. Prolonged application of the hypo-osmotic solution produced a final volume increase (after 480 s, dotted lines) of 10 ± 1.6 %. (n = 3), which is consistent with a final equilibrium determined by osmotic balance.

The initial slope of these data (3.0 (± 0.5) × 10^{-4} s^{-1}, n = 4) can be used to determine an apparent water permeability, L_p (see Methods). We found a value of L_p = 2.0 (± 0.3) × 10^{-4} cm s^{-1} ($\Delta\pi$ = 30 mosmol kg^{-1}). This value is consistent with water diffusion through lipid bilayers two orders of magnitude less than that implied by the presence of

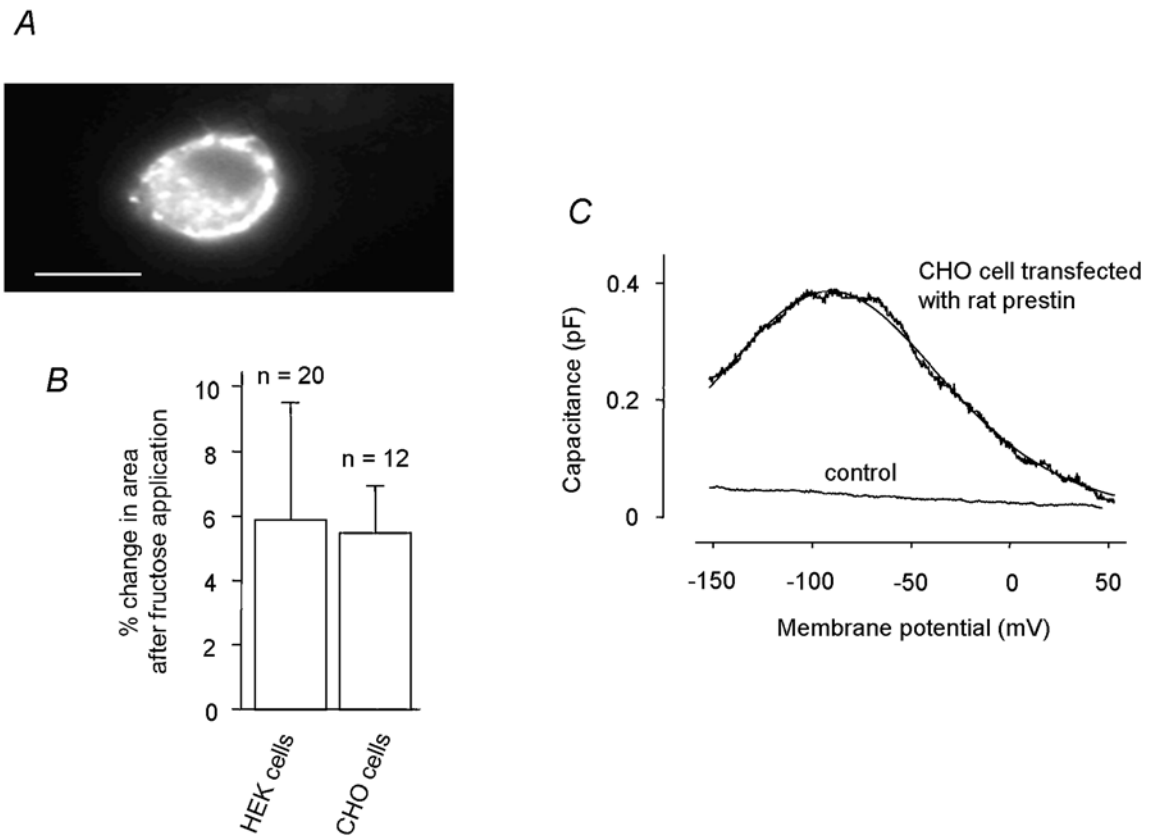

Figure 5. Sugar transport and non-linear capacitance measured in CHO-K1 cells expressing rat prestin

A, CHO-K1 cell expressing the GFP-tagged prestin protein where a membrane translocation is evident. *B*, the two cell types, when transfected, responded indistinguishably: iso-osmotic replacement of glucose with 30 mM fructose does not differ between HEK-293 and CHO-K1 cells. *C*, non-linear capacitance measured with a phase-tracking technique in response to a voltage ramp from −150 to +50 mV. Line is the fit of eqn (3) to data with values for the fit parameters of −90 mV ($V_{1/2}$) and 39 mV (α). Capacitance measured relative to the linear capacitance C_{lin}.

significant levels of water channels in the membrane (Verkman & Mitra, 2000). It is also consistent with values of L_p reported for passive water transport through the sodium-dependent glucose transporter SGLT1 (Loo *et al.* 1999).

Figure 6 shows the comparison of swelling induced by isosmotic replacement of glucose by fructose in the same population of prestin-transfected cells (○, same data set as Fig. 4). The initial rate of cell volume increase ($10 (\pm 1) \times 10^{-4}$ s^{-1}, $n = 20$) was 3.3 times greater than that produced by hypo-osmotic stimulation. In the steady state the cell volume increased to 108 % of the baseline. When the external solution was returned to the control glucose solution, the cell returned to its pre-exposure volume, at almost the same rate. The data are consistent with a rapid movement of fructose across the cell membrane bringing water with it to balance osmotic pressure.

To show coupling between fructose transport and water movement during cell shrinking, transfected cells were equilibrated with a 310 mosmol kg^{-1} (20 mM fructose) solution and then exposed for 200 s to a relatively hyper-osmotic 320 mosmol kg^{-1} (30 mM fructose) solution. Figure 6 (■) shows that the cell volume reduced by 2.4 ± 1.7 % ($n = 5$). The decrease in cell volume indicates that water flowed out of the cell. In this case, where water moved out (following the hyperosmotic stimulus) and fructose moved in (from the fructose gradient) carrying water, the net water flux was outwards.

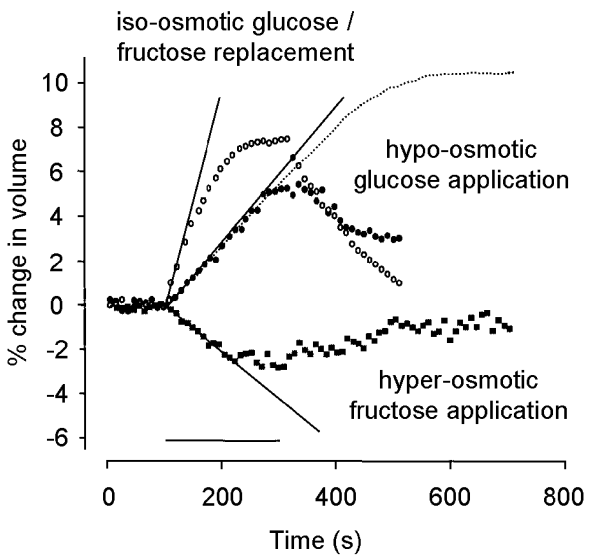

Figure 6. Water movement in HEK-293 cells transfected with rat prestin

Cell swelling caused by isosmotic 30 mM glucose/fructose replacement (○) and 30 mosmol kg^{-1} hypo-osmotic glucose solution application (●). With prolonged hypo-osmotic glucose solution exposure (dotted line), the cell reached a steady state. Cell shrinking was caused by hyperosmotic fructose solution application (■). The cell was equilibrated in 20 mM fructose solution and then exposed to 10 mosmol kg^{-1} hyperosmotic solution containing 30 mM fructose. Although the cell volume decreased, the water permeability (L_p) was the same as in isosmotic fructose replacement. In all cases, the superimposed straight lines are a linear fit through the rising phase of the volume response and the horizontal bar indicates the timing of the application (200 s).

Consistent with the hypothesis that fructose is responsible for dragging water with each transported molecule, the net volume change was less than that obtained with comparable hyper-osmotic stimuli. Untransfected cells were equilibrated with a 310 mosmol kg^{-1} (20 mM fructose) solution and then exposed for 200 s to a relatively hyperosmotic stimulus (320 mosmol kg^{-1}, 30 mM fructose). The cell volume decreased by 3.5 ± 2.7 % ($n = 5$, data not shown). The inferred L_p was $5 (\pm 2) \times 10^{-4}$ cm s^{-1}. This L_p is slightly larger than that found for transfected cells. There was no significant difference in measured geometric membrane area (which also enters into the determination of L_p) between transfected and untransfected cells in the resting state. The results may indicate that prestin transfection could have altered the permeability of the native membrane or, more probably, that small diameter changes were more poorly resolved using DIC optics than using fluorescence.

Sugar transport by other SLC26A transporters

Prestin (SL26A5) belongs to a new and distinct family of solute carriers, SLC26, that includes pendrin (SLC26A4). This latter protein is expressed in the stria vascularis of the cochlea and is mutated in some forms of hereditary hearing loss. We expressed the pendrin construct tagged with GFP in HEK-293 cells to investigate whether this protein also transported sugars. Figure 7*A* shows that GFP-tagged human pendrin displayed a similar behaviour to rat prestin when transfected in HEK-293 cells and exposed to a subset of sugars.

On replacement of glucose with fructose and mannose, pendrin-transfected cells were found to swell by 7.6 ± 4.8 % ($n = 12$) and 5.4 ± 3.7 % ($n = 4$), respectively (Fig. 7*B*). This was more than that found with prestin-transfected cells and shows that pendrin is also capable of using mannose and fructose as a substrate for transport.

Presence of modifying molecular co-factors of prestin in cell lines

To check whether fructose was being carried through native fructose transporters in the cell lines we used, the presence of mRNA coding for GLUT5 was assayed using RT-PCR. Using appropriately designed primers (see Methods) and controls, we found no evidence for the presence of mRNA coding for this fructose transporter in our samples of HEK-293 or CHO cells.

DISCUSSION

Sugar transport in cochlear OHCs

The results presented here indicate that at least two members of the SLC26 family of anion transporters are able to act as sugar transporters. For the range of substrates tested, the properties coincide with those of members of the SLC2 superfamily of glucose transporters that transport fructose (Joost & Thorens, 2001). SLC26A5 (prestin) is specifically expressed in OHCs (Zheng *et al.* 2000) and exhibits motor properties when expressed heterologously in mammalian cell lines. It shows both charge movement and electromotility characteristic of the OHC motor protein. It has recently been reported that prestin knockout mice do not exhibit characteristics associated with functional OHCs (Liberman *et al.* 2002), data which point to the essential role played by prestin in the OHC electromotive process.

The basolateral membrane of OHCs, which expresses high levels of prestin, also transports sugars (Géléoc *et al.* 1999). The kinetics of this transport are similar (although not identical) to that of GLUT5, a high-affinity fructose transporter but with a lower capacity to transport glucose (Burant *et al.* 1992; Rand *et al.* 1993). Antibodies raised against the last 12 C-terminal amino acids of GLUT5 label the basolateral membrane of the OHCs (Nakazawa *et al.* 1995; Belyantseva *et al.* 2000*a*). Géléoc *et al.* (1999) showed that the replacement of extracellular glucose by fructose not only led to reversible cell morphology changes indicative of sugar transport but also induced a shift in the bell-shaped non-linear capacitance curve of the cell. These data suggest that a sugar transporter in OHCs is implicated in OHC electromotility.

The data here show that the prestin protein, as well as presenting electromotive properties, can transport sugars. Since salicylate blocked sugar transport in prestin-transfected cells and since salicylate blocks charge transfer and electromotility (Tunstall *et al.* 1995; Zheng *et al.* 2000), we suggest that sugar transport by prestin is closely linked to the protein conformational change that underlies electromotility. Even though DIDS is reported to inhibit chloride–bicarbonate exchange in SL26A9 (Lohi *et al.* 2002), DIDS had no effect on sugar transport in prestin-transfected cells. The different effect of salicylate and DIDS may suggest that the transport mechanisms of anions and of sugars by prestin could be distinct.

Although it could be concluded that prestin accounts for all the GLUT5-like properties of OHC sugar transport, it is still not possible to rule out the formation of a complex of prestin with several other as yet unidentified subunits. In this case each subunit could act as a cofactor for the motor protein, sensitive to the intracellular anion concentration. The resulting multimeric structures could form a central pore allowing the transport of the non-charged molecules.

Other glucose transporters such as GLUT1, localised in vascular endothelial cells and neuronal satellite cells, and GLUT4 have not been detected in the cochlea (Ito *et al.* 1993). Although RT-PCR shows that GLUT5 is absent in both HEK-293 and CHO cells, the possibility of another unknown member of the GLUT family cannot be excluded. It could be imagined that such a novel transporter might be able to form a functional transport complex with prestin. Nevertheless, since non-transfected cells did not exhibit any detectable sugar transport, the most economical hypothesis seems to be that a single prestin molecule, with a defined stoichiometry, is sufficient to work as a sugar transporter.

Aquaporins could, in principle, also form a complex with prestin or pendrin. Aquaporin proteins are involved in water transport (Verkman & Mitra, 2000) in a wide variety of tissues. The aquaporin family has 10 members and one of these members is present in HEK-293 cells (Dohke & Turner, 2002) and in CHO cells (Van Hoek *et al.* 1998).

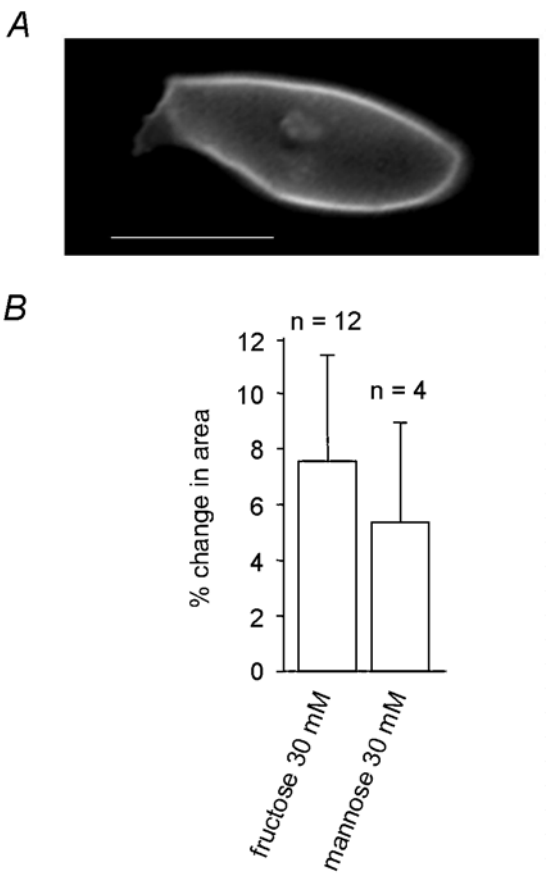

Figure 7. Sugar uptake by HEK-293 cells expressing the pendrin protein

A, HEK-293 cell expressing the GFP-tagged pendrin protein. *B*, change in cell area following isosmotic replacement in the bathing solution of 30 mM glucose by 30 mM fructose or 30 mM mannose. Scale bar, 10 μm.

Thus these proteins could play a role in maintaining the osmotic balance after sugar entry. The value of L_p found in transfected HEK-293 cells (2×10^{-4} cm s^{-1}) indicates that the expression levels of aquaporins are likely to be low. A value of L_p of the order of 10^{-2} cm s^{-1} would indicate, unequivocally, aquaporin-mediated water transport (Verkman & Mitra, 2000).

The values obtained here for the L_p are comparable to those reported for the membrane of neonatal rat OHCs (5×10^{-4} cm s^{-1}; Belyantseva *et al.* 2000*b*). The adult rat value of L_p obtained in OHCs (9.7×10^{-3} cm s^{-1}) is approximately 30 times greater than that obtained using osmotic stimuli. Since the expression level of prestin in adult rat OHCs is about 20–30 times greater than found in our expression systems, and since L_p measures the volume flow per unit area, the simplest hypothesis is that water is carried through the prestin molecule in the cell membrane in OHCs as well as in transfected HEK-293 and CHO cells. In addition, OHC water transport has been demonstrated to be voltage dependent in OHCs (Géléoc *et al.* 1999; Belyantseva *et al.* 2000*b*). It seems most probable that effect is a consequence of the voltage dependence of the SLC26A5 voltage-dependent transport cycle.

The single molecule transport rates

The cell swelling rate can be used to estimate the number of sugar molecules transported across the membrane by a single prestin molecule per second. The simplest assumption is that the volume increase reflects an influx of sugar and that solute osmotic pressure is maintained across the membrane by water brought into the cell. If we assume a cell volume of 4 pl, the measured transport rate, until osmotic equilibrium was reached, corresponds to approximately 3080 fructose molecules (prestin molecule)$^{-1}$ s^{-1}. If the motor protein forms a multimer (e.g. a tetramer) rather than a monomer, and if the multimer were to form the sugar transport pore, the number of sugar molecules transported per prestin molecule would be reduced by the motor stoichiometry. For example, if the stoichiometry is 4, then the transport rate would be 750 fructose molecules (prestin molecule)$^{-1}$ s^{-1}.

If we further assume that all the water flows through the transporter in transfected cells we find that the volume flow of water produced by osmotic stimuli is

$$4 \text{ pl} \times 0.001 \text{ s}^{-1}/250\,000 = 16 \text{ zl (prestin molecule)}^{-1} \text{ s}^{-1}$$

where 1 zl = 10^{-21} l. This number is the same order of magnitude as that found for water movement through SGLT1 in oocytes (3.8 zl transporter^{-1} s^{-1}; Loo *et al.* 1999) where a different method of estimating transporter number was used. Converting this value to a flux of water molecules (= 16 zl $\times$ N/V_W, where N is Avogadro's number), we find that about 175 water molecules would have been transported with each fructose molecule. This number must represent an upper limit. If not all the water flow equilibrated through the transporter but flowed, for example, through a low level of aquaporins in the membrane, or even passively through prestin itself as suggested by the data of Fig. 6, this estimate would be reduced. For example, assuming that the osmotically induced flow (Fig. 6, ●) is passing through an aquaporin and that the excess water flow is via prestin, the water associated with prestin-transported fructose would be $175 \times (3.3 - 1)/3.3 = 120$ water molecules (fructose molecule)$^{-1}$. Despite the approximate nature of the calculation, this number is consistent with that described for sugar transport in other systems (Fischbarg *et al.* 1990).

In OHCs sugar transport across the membrane is affected by membrane potential (Géléoc *et al.* 1999). All the experiments in this study were carried out at the resting membrane potential measured via electrophysiology (-56 ± 3 mV, $n = 3$). We have not investigated under voltage clamp whether the sugar transport rate can be modified in transfected cells as the expression level was too low. It would be predicted to be voltage dependent. However, it is clear that, in principle, the movement of solutes and water controlled by membrane potential could be a route by which OHCs control their internal pressure and hence the forces that they exert in cochlear mechanics.

The SLC26A family and sugar transport

Both prestin and pendrin are present in the cochlea. Pendrin (SLC26A4) is present in the stria vascularis of the cochlea where it may function as an iodide/chloride transporter (Scott *et al.* 1999). The electromotility of this protein when transfected in a cell line has not been investigated but we have shown here that pendrin, like prestin, is also a sugar transporter in its own right. The transport rate for mannose for both prestin and pendrin is close to the rate for fructose (Figs 3*A* and 7*B*). This difference is not apparent in OHCs where these two sugars differ in their ability to produce shape changes (Géléoc *et al.* 1999). The present data indicate that the interaction domain of the sugar as well as structural rearrangements in SLC26A5 await identification to explain how this protein acts as a motor in OHCs.

REFERENCES

Asano T, Shibasaki Y, Ohno S, Taira H, Lin JL, Kasuga M, Kanazawa Y, Akanuma Y, Takaku F & Oka Y (1989). Rabbit brain glucose transporter responds to insulin when expressed in insulin-sensitive Chinese hamster ovary cells. *J Biol Chem* **264**, 3416–3420.

Ashmore JF, Géléoc GS & Harbott L (2000). Molecular mechanisms of sound amplification in the mammalian cochlea. *Proc Natl Acad Sci U S A* **97**, 11759–11764.

Belyantseva IA, Adler HJ, Curi R, Frolenkov GI & Kachar B (2000*a*). Expression and localisation of prestin and the sugar transporter GLUT-5 during development of electromotility in cochlear outer hair cells. *J Neurosci* **20**, RC116, 1–5.

Belyantseva IA, Frolenkov GI, Wade JB, Mammano F & Kachar B (2000*b*). Water permeability of cochlear outer hair cells: characterisation and relationship to electromotility. *J Neurosci* **20**, 8996–9003.

Burant CF, Takeda J, Brot-Laroche E, Bell GI & Davidson NO (1992). Fructose transporter in human spermatozoa and small intestine is GLUT5. *J Biol Chem* **267**, 14523–14526.

Dohke Y & Turner RJ (2002). Evidence that the transmembrane biogenesis of aquaporin 1 is cotranslational in intact mammalian cells. *J Biol Chem* **277**, 15215–15219.

Everett LA, Morsli H, Wu DK & Green ED (1999). Expression pattern of the mouse ortholog of the Pendred's syndrome gene (Pds) suggests a key role for pendrin in the inner ear. *Proc Natl Acad Sci U S A* **96**, 9727–9732.

Fischbarg J, Kuang KY, Vera JC, Arant S, Silverstein SC, Loike J & Rosen OM (1990). Glucose transporters serve as water channels. *Proc Natl Acad Sci U S A* **87**, 3244–3247.

Gale JE & Ashmore JF (1997). An intrinsic frequency limit to the cochlear amplifier. *Nature* **389**, 63–66.

Géléoc GS, Casalotti SO, Forge A & Ashmore JF (1999). A sugar transporter as a candidate for the outer hair cell motor. *Nat Neurosci* **2**, 713–719.

Ito M, Spicer SS & Schulte BA (1993). Immunohistochemical localisation of brain type glucose transporter in mammalian inner ears: comparison of developmental and adult stages. *Hear Res* **71**, 230–238.

Joost HG & Thorens B (2001). The extended GLUT-family of sugar/polyol transport facilitators: nomenclature, sequence characteristics, and potential function of its novel members. *Mol Membr Biol* **18**, 247–256.

Kim DK, Kanai Y, Matsuo H, Kim JY, Chairoungdua A, Kobayashi Y, Enomoto A, Cha SH, Goya T & Endou H (2002). The human T-type amino acid transporter-1: characterization, gene organization, and chromosomal location. *Genomics* **79**, 95–103.

Kurata T, Oguri T, Isobe T, Ishioka S & Yamakido M (1999). Differential expression of facilitative glucose transporter (GLUT) genes in primary lung cancers and their liver metastases. *Jpn J Cancer Res* **90**, 1238–1243.

Liberman MC, Gao J, He DZZ, Wu X, Jia S & Zuo J (2002). Prestin is required for electromotility of the outer hair cell and for the cochlear amplifier. *Nature* **419**, 300–304.

Lohi H, Kujala M, Kerkela E, Saarialho-Kere U, Kestila M & Kere J (2000). Mapping of five new putative anion transporter genes in human and characterization of SLC26A6 a candidate gene for pancreatic anion exchanger. *Genomics* **70**, 102–112.

Lohi H, Kujala M, Makela S, Lehtonen E, Kestila M, Saarialho-Kere U, Markovich D & Kere J (2002). Functional characterization of three novel tissue-specific anion exchangers SLC26A7, -A8, and -A9. *J Biol Chem* **277**, 14246–14254.

Loo DDF, Hirayama BA, Meinild A-K, Chandy G, Zeuthen T & Wright EM (1999). Passive water and ion transport by cotransporters. *J Physiol* **518**, 195–202.

Ludwig J, Oliver D, Frank G, Klocker N, Gummer AW & Fakler B (2001). Reciprocal electromechanical properties of rat prestin: the motor molecule from rat outer hair cells. *Proc Natl Acad Sci U S A* **98**, 4178–4183.

Nakazawa K, Spicer SS & Schulte BA (1995). Postnatal expression of the facilitated glucose transporter GLUT 5 in gerbil outer hair cells. *Hear Res* **82**, 93–99.

Neher E & Marty A (1982). Discrete changes of cell membrane capacitance observed under conditions of enhanced secretion in bovine adrenal chromaffin cells. *Proc Natl Acad Sci U S A* **79**, 6712–6716.

Oliver D, He DZ, Klocker N, Ludwig J, Schulte U, Waldegger S, Ruppersberg JP, Dallos P & Fakler B (2001). Intracellular anions as the voltage sensor of prestin, the outer hair cell motor protein. *Science* **292**, 2340–2343.

Rand EB, Depaoli AM, Davidson NO, Bell GI & Burant CF (1993). Sequence, tissue distribution, and functional characterisation of the rat fructose transporter GLUT5. *Am J Physiol* **264**, G1169–1176.

Scott DA, Wang R, Kreman TM, Sheffield VC & Karniski LP (1999). The Pendred syndrome gene encodes a chloride–iodide transport protein. *Nat Genet* **21**, 440–443.

Tunstall MJ, Gale JE & Ashmore JF (1995). Action of salicylate on membrane capacitance of outer hair cells from the guinea-pig cochlea. *J Physiol* **485**, 739–752.

Van Hoek AN, Yang B, Kirmiz S & Brown D (1998). Freeze-fracture analysis of plasma membranes of CHO cells stably expressing aquaporins 1–5. *J Membr Biol* **165**, 243–254.

Verkman AS & Mitra AK (2000). Structure and function of aquaporin water channels. *Am J Physiol Renal Physiol* **278**, F13–28.

Waldegger S, Moschen I, Ramirez A, Smith RJ, Ayadi H, Lang F & Kubisch C (2001). Cloning and characterization of SLC26A6 a novel member of the solute carrier 26 gene family. *Genomics* **72**, 43–50.

Zeuthen T, Meinild AK, Loo DD, Wright EM & Klaerke DA (2001). Isotonic transport by the Na^+-glucose cotransporter SGLT1 from humans and rabbit. *J Physiol* **531**, 631–644.

Zheng J, Shen W, He DZ, Long KB, Madison LD & Dallos P (2000). Prestin is the motor protein of cochlear outer hair cells. *Nature* **405**, 149–155.

Acknowledgements

We thank H. Dorricott for technical assistance, Dr B. Fakler for kindly providing the plasmid containing rat prestin and Dr R. Trembath for the gift of the pendrin construct. We also thank B. Perez Mansilla and G. Thomas for their help with radioactive transport experiments and A. Gardner-Medwin for comments on the manuscript. This work was supported by the Wellcome Trust.